33RD CONGRESS
OF THE INTERNATIONAL COUNCIL
OF THE AERONAUTICAL SCIENCES
STOCKHOLM, SWEDEN, 4-9 SEPTEMBER, 2022

ICAS 2022 SWEDEN

COMPUTATIONALLY ECONOMICAL METHODS FOR LANDING GEAR NOISE SIMULATION

Robert Spencer[1] & Mark Allan[2]

[1]CFMS, Bristol, UK. robert.spencer@cfms.org.uk
[2]Zenotech Ltd, Bristol, UK. mark.allan@zenotech.com

Abstract

Aircraft landing and take-off noise is subject to stringent legislation. Landing gear generates a large proportion of landing noise, so minimising landing gear noise is of significant industrial interest. Unfortunately, traditional aero-acoustic simulation methods based on high quality scale resolving simulations are expensive and time-consuming, limiting their application within the design loop. In this paper, two aero-acoustic simulation methodologies which are more economical to run than conventional scale resolving simulations are applied to the PDCC-NLG landing gear acoustic test case. First, an implicit LES simulation using an Octree castellated mesh with no grown boundary layer mesh is used. Secondly, a stochastic simulation using the Fast Random Particle Method (as implemented in the zCFD flow solver) is used. Both simulations are compared to experimental data and previously published scale resolving simulations.

Keywords: CFD, Landing Gear, Acoustics, FRPM, LES, Meshing

1. Introduction

Surveys have consistently shown that aircraft noise is the aspect of airport operations which causes nearby residents the greatest annoyance [1], and there is also evidence of an adverse impact on nearby resident's health [2]. It is therefore unsurprising that landing and take-off noise are subject to stringent, and ever-tightening, regulations [3, 4]. As engine bypass ratios have increased, engine noise has reduced, meaning landing gear now contributes a larger proportion of the total aircraft noise [3, 5].

While landing gear can to some extent be streamlined [6, 7], the wheels mean that the flow field will always involve large bluff bodies, which make analysis and optimisation of the landing gear's noise signature difficult and expensive [8]. A traditional approach to predicting landing gear noise involves high fidelity scale-resolving simulations [9, 8]. Unfortunately, this simulation type is complex, time-consuming and expensive, meaning it is unlikely to form part of the 'design-test-improve' iterative design cycle. Instead, high fidelity aero-acoustic simulations are currently more likely to be used as part of a research project, or as part of a pass off test on a design nearing finalisation.

The limited use of acoustic simulations in the iterative design cycle means that acoustic performance currently acts as a design 'output', as opposed to an active design variable which can be optimised during the design cycle. It is therefore of high industrial interest to develop acoustic performance prediction methods which are fast, economical and robust enough to form part of the iterative design cycle. Acoustic simulations which were sufficiently fast and robust could even appear in automated design optimisation loops, reducing design cycle time and possibly leading to innovative new landing gear designs.

In this paper, two computational methods ('Octree LES' and 'FRPM' [10]) which are fast enough to use as part of the iterative design cycle are used to predict the noise signature of the PDCC-NLG (Partially Dressed Closed Cavity - Nose Landing Gear) landing gear test case. The efficiency improvements from the 'Octree LES' approach are a result of both reduced user time spent on meshing

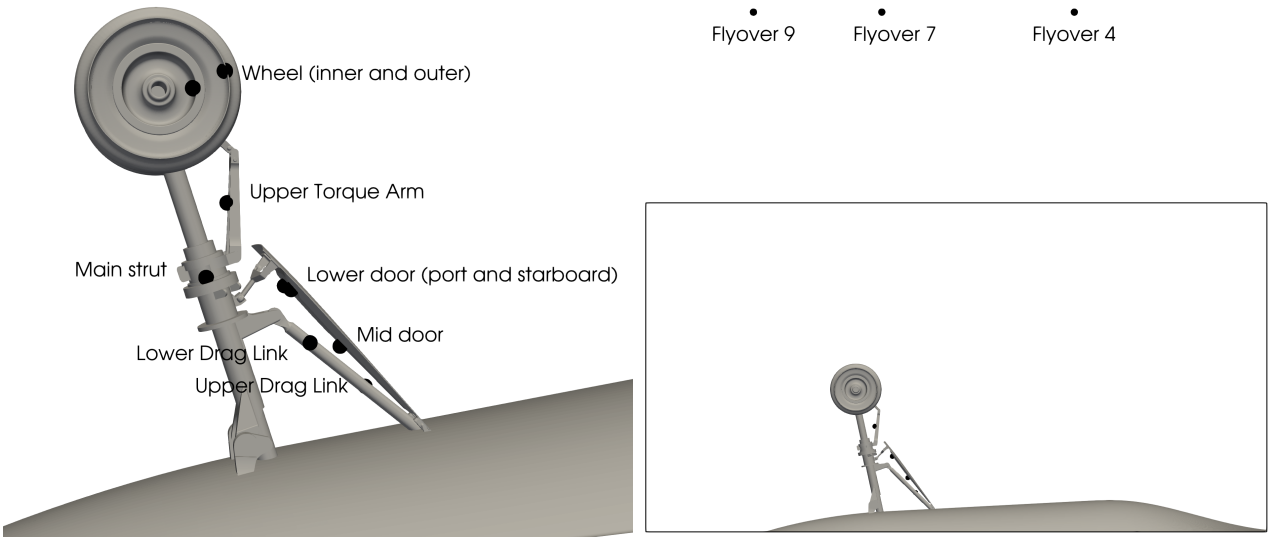

Figure 1 – Acoustic probe locations

and increased computational efficiency. The 'FRPM' method is a stochastic technique that augments steady state RANS data to provide time-varying acoustic sources at reduced computational cost. The aim of both of these methods is to be sufficiently accurate to allow comparison of the acoustics of different candidate designs, but also fast enough to be used in the design cycle.

2. Simulations

2.1 Test case setup

The PDCC-NLG test case is based on a 1/4 scale Gulfstream G550 nose landing gear, was first proposed by Khorrami [11] [12] and has been used as part of a BANC workshop [13]. Experimental data [14, 15] and several simulations [16, 17] of this test case have been published. There are two versions of this test case (matching the conditions at two different wind tunnels), and the simulations presented in this work use the Track A (BART) conditions. The freestream Mach number is therefore 0.166, and the Reynolds number based on the shock strut diameter is 73,000.

Acoustic simulations of this test case are normally assessed by comparing acoustic spectra at a series of near and far-field probe locations to experimental data. The placement of the acoustic probes considered in this work are shown in Figure 1. While more probes are considered in the original experimental dataset [14], the subset used in this work are those which are most commonly reported in the literature. The probe names used in this work follow that used by Van de Ven et al. [16] (as opposed to the slightly different convention used by Neuhart et al. [14]).

The near-field probe experimental data was collected using the Track A (BART) experimental setup, which used a regular, rectangular cross-section wind tunnel. However, the far-field ('flyover') probes were collected using the Track B (UFAFF) experimental setup, which instead used an open jet acoustic wind tunnel. This means that there is a shear layer between the flyover probes and the landing gear in the experiment, and also that a simulation using the Track A configuration cannot include the flyover probes in its mesh because they extend beyond the BART tunnel's wall. Therefore, in this work flyover data was calculated using 'traced back' probes, which lie inside the mesh on the line between the wheels (judged as the main noise-generating region) and the 'official' flyover probe locations, and by using inverse scaling to infer the flyover probe noise. Farfield data was only collected for the FRPM simulation, since the Octree LES mesh was not fine enough in the farfield to transmit acoustic waves of the required frequency. Future work may include the use of an FWH solver to calculate farfield noise using the LES simulations.

2.2 Octree LES

While Moore's law and widespread access to HPC have drastically reduced the cost and wall clock time of a given CFD simulation over the last 30 years, mesh generation has not experienced a similar productivity increase over the same time period. Lower compute costs mean that scale resolving simulations like LES are becoming relatively commonplace, but the increased mesh sizes they entail mean that meshing is becoming a bottleneck in the CFD practitioner's workflow [18, 19]. In the absence of a significant breakthrough in meshing software, this bottleneck is likely to get worse in the future as computational costs get lower and mesh counts get ever larger.

In a conventional unstructured CFD meshing algorithm, a large part of the meshing time (and a common reason for mesh builds to fail) is taken up in the creation of the body-fitted 'inflation' layer, and in matching this layer to the far-field mesh [20]. The inflation layer exists in order to accurately resolve the boundary layer, which is important for skin friction and therefore drag prediction, particularly in streamlined bodies. However, in high Reynolds number flow over bluff bodies like landing gear, pressure drag (as opposed to friction drag) is the dominant source of drag, making prediction of skin friction less important (especially in acoustic simulations where drag prediction is not the primary objective).

Therefore, the approach taken in the 'Octree LES' method is to use an LES simulation, but forego the boundary fitted inflation layer entirely, instead using a cartesian aligned Octree mesh which is refined (sub-divided) to a prescribed level at the geometry. This has implications for boundary layer prediction accuracy, but has the large advantages of speed, simplicity and robustness. This approach is also particularly suited to LES, where isotropic cells are required for accurate sub grid modelling. Removing the inflation layer means that the meshing algorithm becomes simpler to code and far more robust (especially for complex geometries), and there are less meshing parameters for the user to spend time setting. As compute costs become lower, the inaccuracies in boundary layer prediction that result from this method can be mitigated by simply increasing near wall mesh density. The use of LES, a scale resolving simulation type, means that acoustic data can be collected.

As well as simplifying meshing, removing the inflation layer also means that there are none of the highly anisotropic elements normally seen in the inflation layer. The numerical stiffness associated with boundary layers is therefore reduced, and the minimum timestep associated with stability (for explicit time marching methods) is increased, substantially reducing the computational effort required for the same simulation time.

The Octree LES approach also has some parallels with the approach taken in Lattice-Boltzmann solvers such as PowerFLOW [21]. The Lattice-Boltzmann method means that PowerFLOW uses Octree meshes with no inflation layer by necessity, and PowerFLOW is generally regarded as most suitable for unsteady, geometrically complex and massively separated flows [21].

Two 'Octree LES' simulations are presented in this work - a baseline simulation and a fine version with a finer near wall mesh resolution. An overview of the baseline mesh is shown in Figure 2, and detail of both baseline and fine meshes is shown in Figure 3, showing detail of the castellation at the boundary. At present no attempt is made to project the boundaries of cells to the geometry (which would remove the surface castellation), although this is a relatively simple process. As such, the mesh can be considered as providing an inherent roughness of the order of the prescribed cell dimension.

The mesh used in the current work is based on that used by Mendonça [22] in their StarCCM simulation of the PDCC-NLG case, but without the wall inflation layer. The meshing strategy used by Mendonça is more fully described in his paper [22], but briefly consists of three refinement regions (as shown in Figure 2). In the Octree LES simulations, the maximum cell sizes in these regions were 12 mm, 6 mm and 1.5 mm respectively. The mesh used by Mendonça [22] had 37 million cells, while the baseline and fine meshes used in this work (see Figures 2 and 3) had 48 and 58 million cells respectively. The only difference between the baseline and fine versions of the Octree LES simulations is that the fine simulation used a finer near wall resolution of 0.375 mm as opposed to 0.75 mm (see Figure 3).

The Octree LES simulations were implicit LES simulations, where the dissipation inherent to the discretisation scheme acts as a subgrid scale model. MUSCL reconstruction was used (which pro-

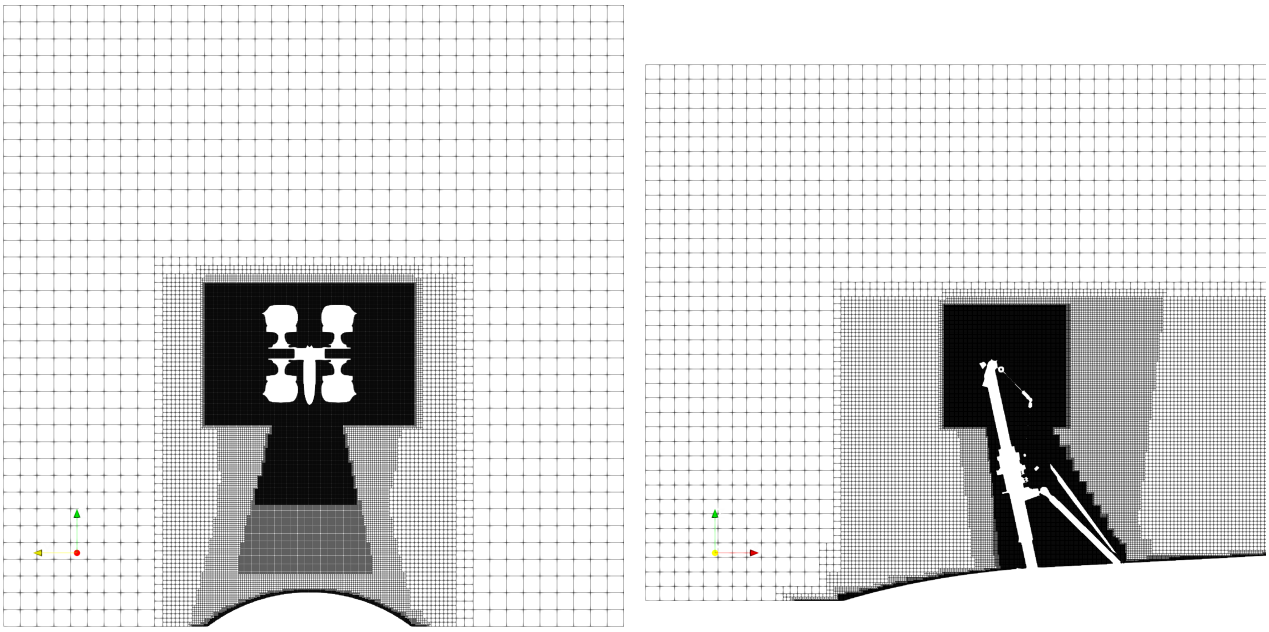

Figure 2 – Octree mesh for implicit LES simulation

vides 3rd order spatial accuracy in cartesian meshes), and the simulations were carried out using the commercial CFD code zCFD [23, 24] . The baseline and fine simulations took 44 and 71 hours respectively on 28 K80 GPU nodes to simulate 0.04 seconds of simulation time.

2.3 FRPM Method

In scale resolving simulations such as LES, the sound-generating turbulence is simulated directly, which requires an expensive time-accurate and finely resolved simulation. The FRPM (Fast Random Particle Method) technique reduces cost by instead modelling sound-generating turbulence stochastically based on turbulence statistics generated by a RANS simulation (which is much less computationally intensive than a scale resolving simulation). Figure 4 (adapted from Grimm et al. [25]) summarises the FRPM simulation procedure.

As described in Figure 4, artificial turbulent fluctuations are generated in a noise generation box chosen by the user, and the fluctuations are transmitted to the far-field via the Acoustic Perturbation Equations (APEs), using an acoustic mesh. The FRPM box and acoustic mesh extents are shown in Figure 5 - the FRPM box encloses the main noise-generating region, while the acoustic mesh extends far enough to contain the traced back flyover probes (see Figure 1).

This method resolves broadband noise only (as opposed to tones), so is not suitable for flows with strong tonal components. The acoustic mesh needs no boundary layer refinement, but its density is set by the wave-length of the highest acoustic frequency to be resolved, so mesh counts can be large when the required sound observer probes are far from the noise generation region. In this case, the FRPM box had cubic cells of side length 6 mm, and a total cell count of 306,800. The acoustic mesh was Octree based with a cell count of 4.8 million, a maximum cell side length of 6.25 mm (therefore resolving a maximum acoustic frequency of 10 kHz), and with a minimum cell size of 3.125 mm at the wall in order to resolve the geometry.

The RANS simulation upon which the FRPM simulation was based used the SST turbulence model, a conventional 36 million node mesh with an inflation layer, and compared quite favourably to the experimental time-mean data. Figure 6 shows a comparison of the RANS vorticity around the wheel to experimental LDV data by Neuhart et al. [14], and Figure 7 compares the pressure coefficient on the gear door to pressure probe data, also by Neuhart et al. [14]. Both show that the RANS is largely able to capture the relevant flow features - the gear door pressure coefficient compares favourably to the LES carried out by Mendonça [22], while the wheel vorticity matches the experimental data less well than the LES by Mendonça [22]. The turbulence integral length scale near the wall was predicted to be around 5 mm by the RANS, which is much larger than the size of the wall castellations in the

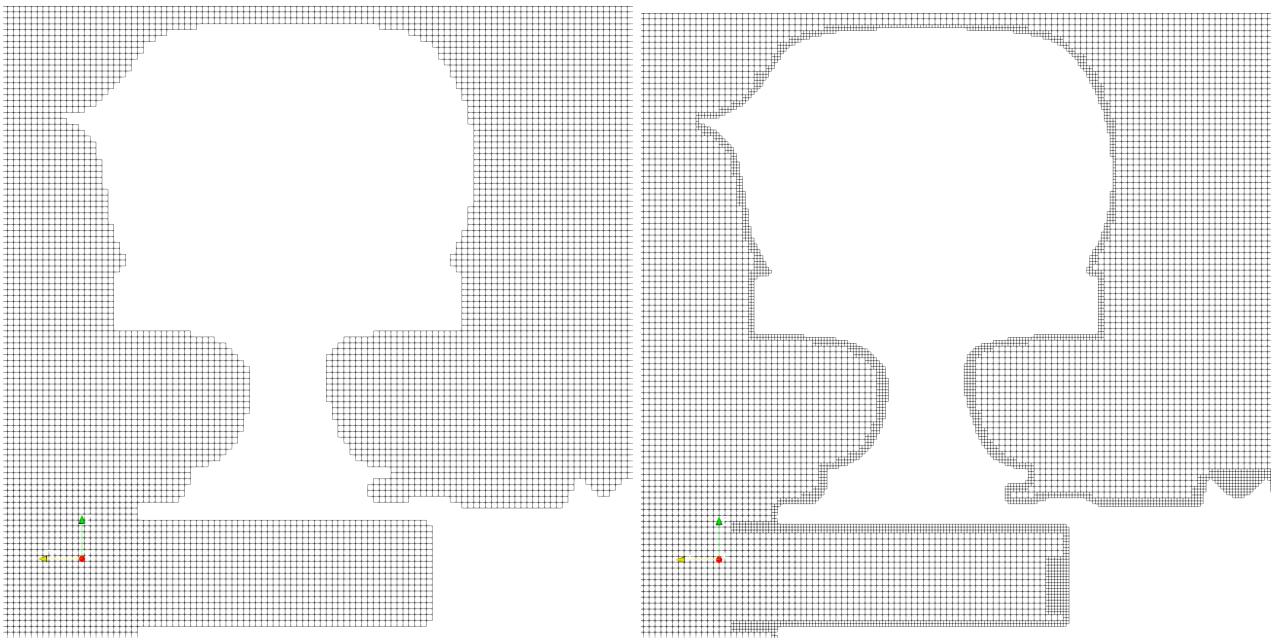

Figure 3 – Close-up of near wall region in Octree meshes (standard left, finer right)

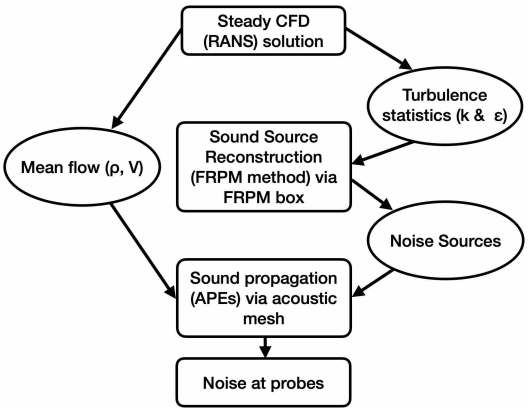

Figure 4 – FRPM simulation flowchart (adapted from Grimm et al. [25])

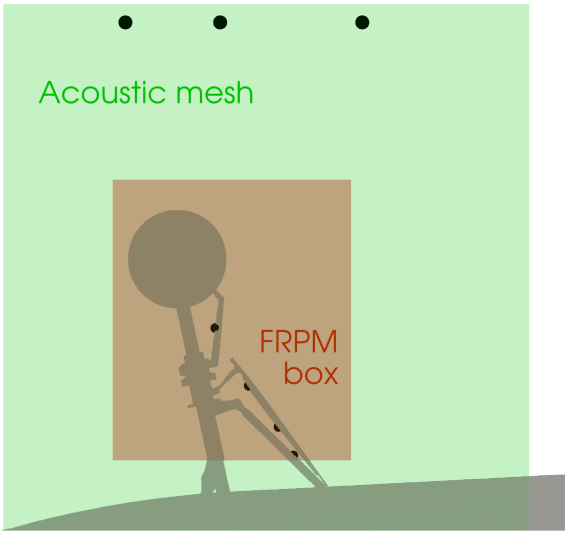

Figure 5 – FRPM simulation noise generation box extent

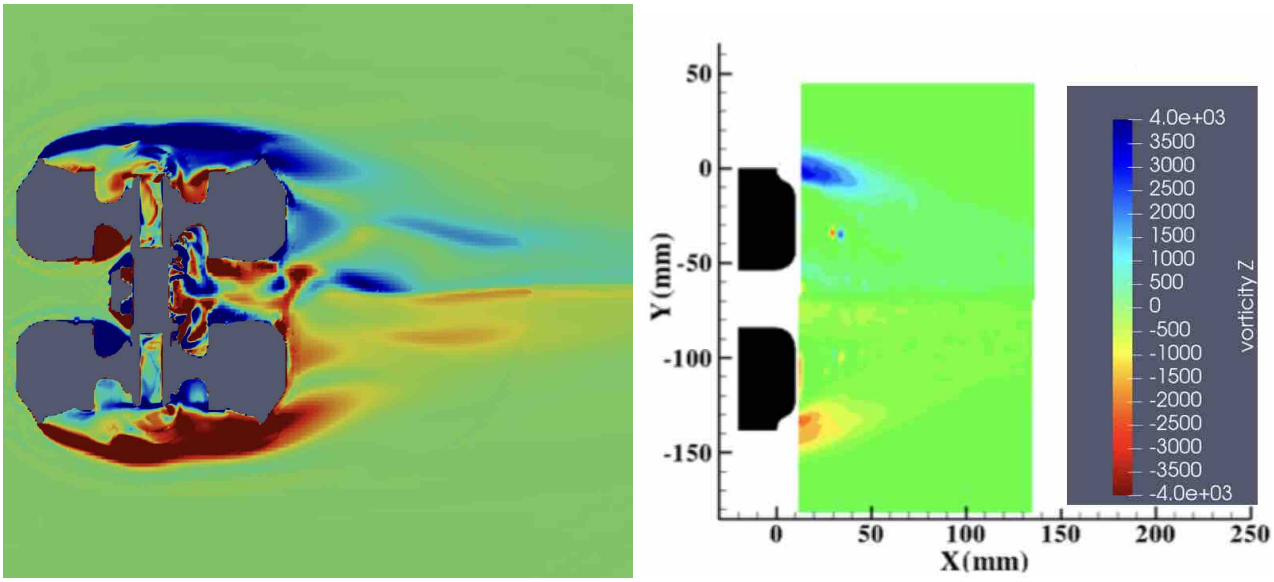

Figure 6 – Wheel wake vorticity - RANS used in FRPM simulation (left) compared to experimental data by [14] (right)

Octree LES mesh. The FRPM simulation was carried out using the commercial CFD code zCFD [23, 24], which has implemented the FRPM method and uses the APE equations to transmit the sound to the farfield. The FRPM/CAA simulation took 12 hours on 20 K80 GPU nodes to simulate 0.2 seconds of simulation time.

3. Results

3.1 Nearfield probes

In Figure 8, nearfield probe acoustic spectra from the zCFD Octree LES and FRPM simulations are compared with experiments, DES and LES simulations by other authors. The StarCCM DES used a mesh with 37 million cells, the Fun3D LES used a mesh with 47 million cells and the baseline and fine zCFD Octree LES simulations presented here used meshes with 48 and 58 million cells respectively. The FRPM simulation used an acoustic mesh with 4.8 million cells. The data has been plotted using a PSD. Raw data was not freely available for the StarCCM or Fun3D simulations, so this data has been digitally extracted from the source papers (note StarCCM and Fun3D data was not available for all probes).

The StarCCM DES gives good results over high and low frequencies on the probes plotted, while the Fun3D LES and zCFD Octree LES tend to fall away from the experimental data at higher frequencies. This is common behaviour for LES, where higher frequencies are modelled as opposed to resolved. As can be seen, the Octree LES performs well. It is generally assumed in the CFD community that resolving the boundary layer is crucial for accuracy, however these simulations, with no boundary layer inflation layer at all and a wall that is not even smooth (due to the castellation of the boundary), gives acoustic prediction accuracy equivalent to results from a boundary-conformal mesh. The fact that the baseline and fine Octree LES simulations lie on top of each other for all probes apart from the upper torque arm suggests that the near wall resolution / roughness is not a significant factor in the accuracy of the acoustic results.

While there is some variability across probes, the only probe which is significantly underpredicted in the zCFD Octree LES results is the main strut - inspection of Figure 1 shows that this probe is out in the freestream, upstream of any significant shedding. This probe is therefore likely sensitive to freestream turbulence settings, and also likely to be the probe most sensitive to boundary layer prediction accuracy (since it is not downstream of a bluff body). The zCFD FRPM nearfield results offer similar accuracy to the LES / DES simulations across all nearfield probes.

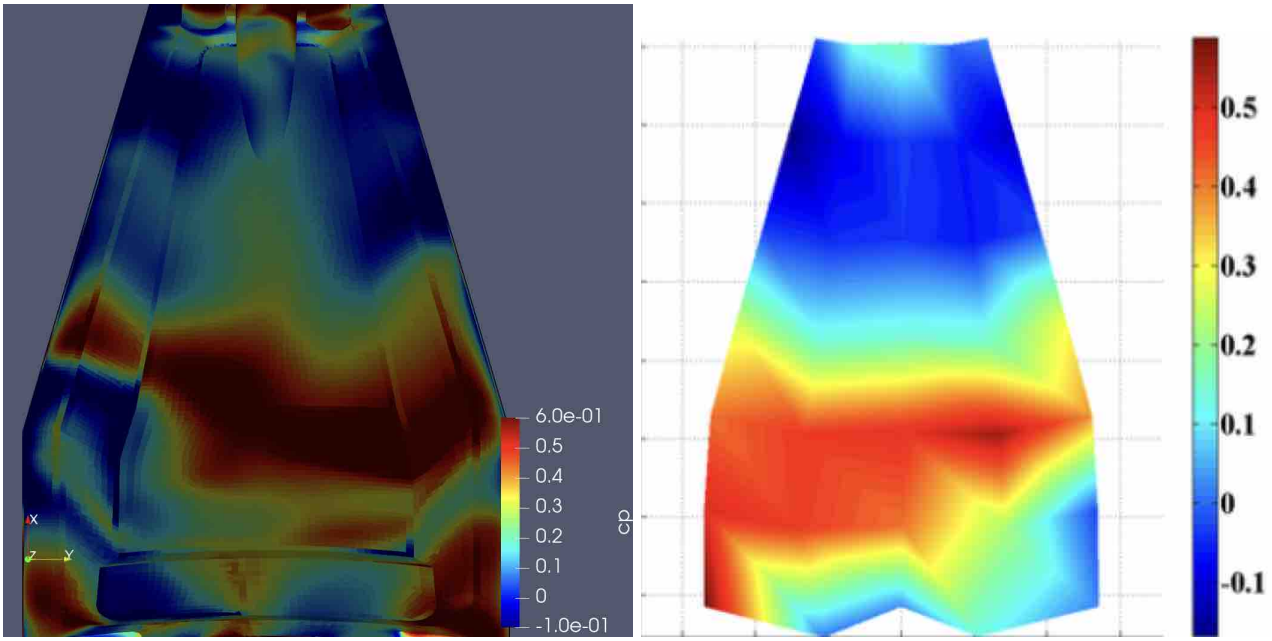

Figure 7 – Gear door pressure coefficient - RANS used in FRPM simulation (left) compared to experimental data by [14] (right)

3.2 Farfield probes

In Figure 9 acoustic spectra at the farfield probes are compared for experiments, a Fun3D LES simulation [17] and the zCFD FRPM simulation from this work. The data is plotted using third-octave bands, using a different frequency range to Figure 8, in order to match the experimental data. Data for zCFD Octree LES and StarCCM LES was not available at these probes, for the reasons outlined in Section 2.1. As stated in Section 2.1, there were limitations in the way that the FRPM data was extrapolated to the probe points, and the Fun3D LES data similarly suffered from limitations in the farfield data collection - in their case the data was collected using an FWH algorithm via an impermeable FWH surface at the wall, which does not account for all types of sound generation.
While the Fun3D LES data overpredicts lower frequencies and underpredicts higher frequencies, the zCFD FRPM data is much more accurate and is particularly impressive given that the zCFD FRPM data underpredicted high frequency noise at the nearfield probes (see Figure 8). This to some extent corroborates the view put forward by Manoha et al. [26], that small energetic structures at low velocity do not radiate farfield noise, and therefore it is only the fast large structures in the nearfield which need to be correctly predicted for correct farfield noise prediction.

4. Conclusions

This work outlined two methods for modelling the acoustic performance of landing gear which are faster and more economical to run than the conventional LES normally used for acoustic simulations. The Octree LES simulations performed similarly to a Fun3D LES simulation with a similar mesh count, but the Octree LES method reduces user time spent on meshing, and the lack of highly anisotropic cells in the inflation layer reduces numerical stiffness, which reduces simulation cost. The Octree LES results therefore support the hypothesis that the commonly quoted pros and cons of a Lattice-Boltzmann solver like PowerFLOW (decreased simulation cost, but best suited to bluff body, pressure-drag dominated flows [21]) can to some extent be replicated with a Navier-Stokes based solver using a similar meshing philosophy.
The FRPM method has been shown to provide accurate results for landing gear noise. The fact that the method only requires a RANS solution, not a scale-resolving simulation, provides the opportunity to generate noise predictions during a design cycle. Despite not being scale-resolving, it gave good predictions of farfield radiated noise.
In summary, both Octree LES and FRPM methods provide accurate prediction of landing gear noise, while offering significant potential cost savings relative to the current state of the art.

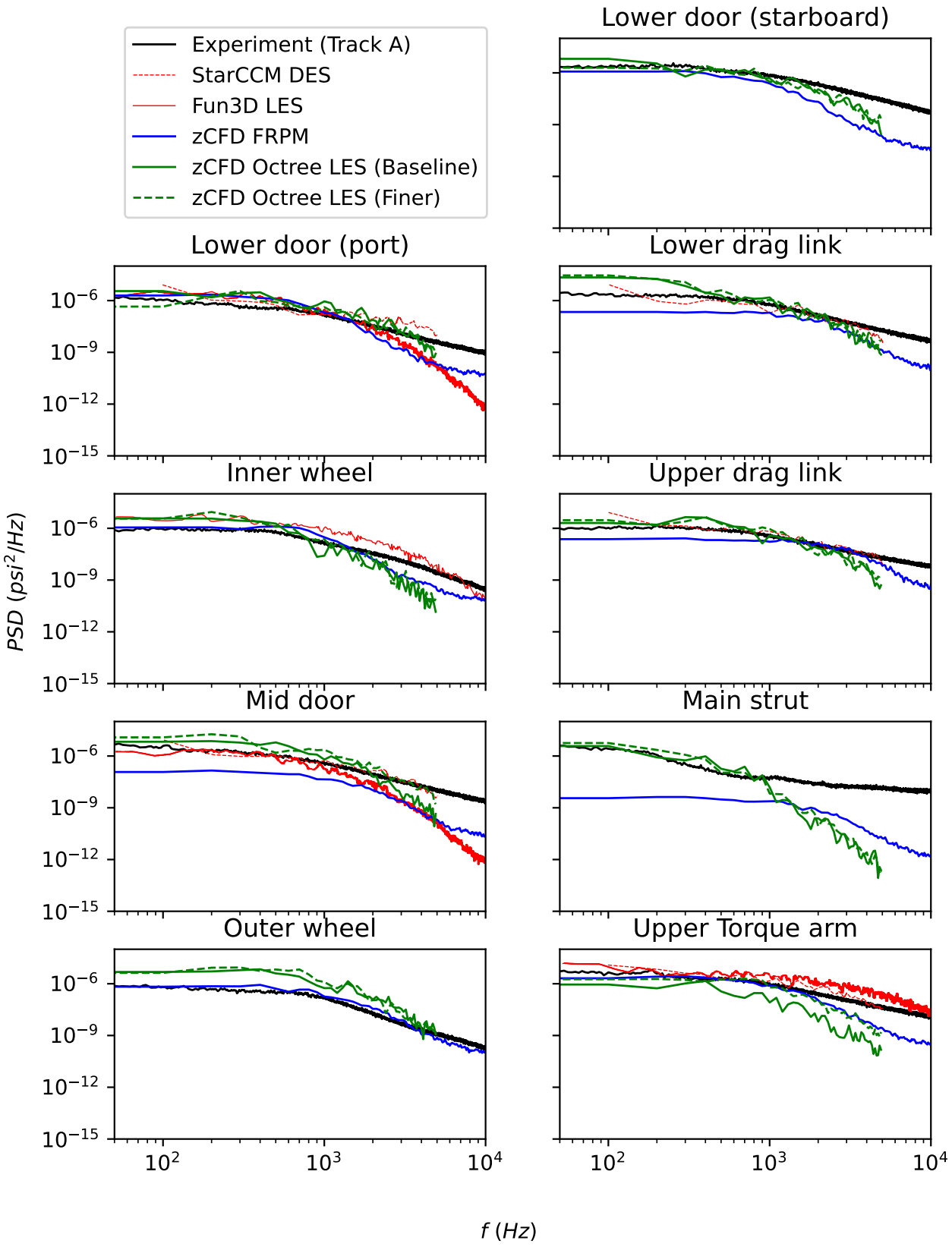

Figure 8 – Near field pressure spectra - Experiments [14] compared with StarCCM DES [16], Fun3D LES [17] and zCFD Octree LES and FRPM (this work)

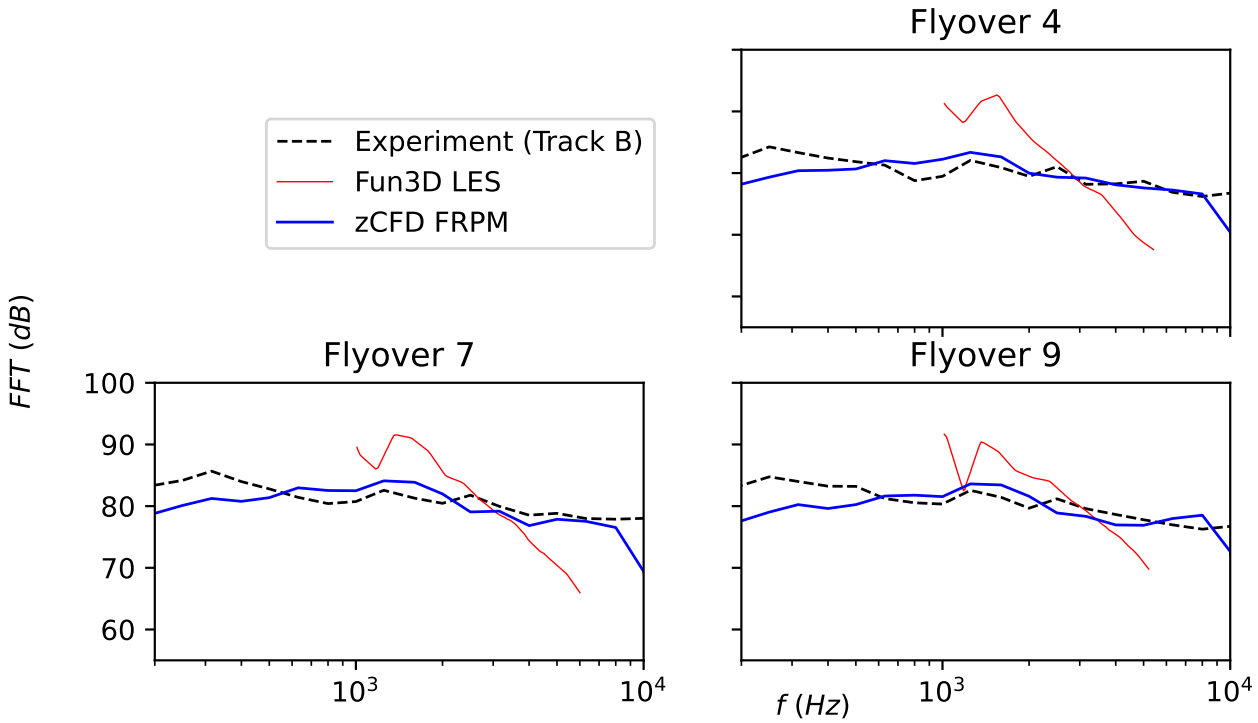

Figure 9 – Flyover pressure spectra - Experiments [14] compared with Fun3D LES [17] and zCFD Octree FRPM (this work)

5. Acknowledgements

This work was carried out as part of the AEROFLUX project, which was funded by the Aerospace Technology Institute (ATI) under contract number 113202.

6. Copyright Statement

References

[1] House of Representatives Report to the Ranking Democratic Member, Committee on Transportation and Infrastructure. Aviation and the environment: Airport operations and future growth present environmental challenges. Technical Report GAO/RCED-00-153, United States General Accounting Office, 2000.

[2] L. Butcher. Aviation noise. Briefing paper SN261, House of Commons Library, 2017.

[3] R. Girvin. Aircraft noise-abatement and mitigation strategies. *Journal of Air Transport Management*, 15:14–22, 2009.

[4] Flightpath 2050: Europe's vision for aviation. Flightpath 2050 europe's vision for aviation report of the high level group on aviation research, Flightpath 2050 Europe's Vision for Aviation, 2011.

[5] O. Zaporozhets, V. Tokarev, and K. Attenborough. *Aircraft noise: Assesment, prediction and control*. Spon Press, 2011.

[6] K. Zhao, P. Okolo, E. Neri, P. Chen, J. Kennedy, and G. Bennet. Noise reduction technologies for aircraft landing gear-a bibliographic review. *Progress in Aerospace Sciences*, 112(100589), 2020.

[7] L. Bertsch, D. G. Simons, and M. Snellen. Aircraft noise: The major sources, modelling capabilities, and reduction possibilities. Workshop executive summary IB 224-2015 A 110, DLR, 2015.

[8] Wen Liu. *Numerical Investigation of Landing Gear Noise*. PhD thesis, University of Southampton, 2011.

[9] Philippe R. Spalart, Mikhail L. Shur, Mikhail Kh. Strelets, and Andrey K. Travin. Initial noise predictions for rudimentary landing gear. *Journal of Sound and Vibration*, 330:4180–4195, 2011.

[10] R. Ewert, J. Dierke, J. Siebert, A. Neifeld, C. Appel, M. Siefert, and O. Kornow. Caa broadband noise prediction for aeroacoustic design. *Journal of Sound and Vibration*, 330:4139–4160, 2011.

[11] Mehdi R. Khorrami and T. Van de Ven. Partially-dressed cavity-closed nose landing gear (pdcc-nlg). Technical report, NASA, Gulfstream, Unknown.

[12] Mehdi R. Khorrami. Toward establishing a realistic benchmark for airframe noise research: Issues and challenges. In *IUTAM Symposium on Computational Aero-Acoustics for Aircraft Noise Prediction*, 2010.

[13] Meelan Choudhari and David Lockard. Simulations and measurements of airframe noise: A banc workshops perspective. Technical Report STO-CfP-AVT-246, NATO OTAN, Unknown.

[14] D. H. Neuhart, Mehdi R. Khorrami, and Meelan Choudhari. Aerodynamics of a gulfstream g550 nose landing gear model. In *15th AIAA/CEAS Aeroacoustics Conference (30th AIAA Aeroacoustics Conference)*, number AIAA 2009-3152, 2009.

[15] N. S. Zawodny, F. Liu, T. Yardibi, L. Cattafesta, Mehdi R. Khorrami, D. H. Neuhart, and T. Van de Ven. A comparative study of a 1⁄4-scale gulfstream g550 aircraft nose gear model. In *15th AIAA/CEAS Aeroacoustics Conference (30th AIAA Aeroacoustics Conference)*, number AIAA 2009-3153, 2009.

[16] T. Van de Ven, J. Louis, D. Palfreyman, and Fred Mendonça. Computational aeroacoustic analysis of a 1⁄4 scale g550 nose landing gear and comparison to nasa and ufl wind tunnel data. In *15th AIAA/CEAS Aeroacoustics Conference (30th AIAA Aeroacoustics Conference)*, number AIAA 2009-3359, 2009.

[17] David P. Lockard Veer N. Vatsa and and Mehdi R. Khorrami. Application of fun3d solver for aeroacoustics simulation of a nose landing gear configuration. In *17th AIAA/CEAS Aeroacoustics Conference (32nd AIAA Aeroacoustics Conference)*, number AIAA 2011-2820, 2011.

[18] J. Slotnick, A. Khodadoust, J. Alonso, D. Darmofal, W. Gropp, E. Lurie, and D. Mavriplis. Cfd vision 2030 study: A path to revolutionary computational aerosciences. Contractor Report NASA/CR–2014-218178, NASA, 2014.

[19] W. N. Dawes, P. C. Dhanasekaran, A. A. J. Demargne, W. P. Kellarn, and A. M. Savill. Reducing bottlenecks in the cad-to-mesh-to-solution cycle time to allow cfd to participate in design. *Journal of Turbomachinery*, 123(552), 2001.

[20] A. A. J. Demargne, R. O. Evans, P. J. Tiller, and W. N. Dawes. Practical and reliable mesh generation for complex, real-world geometries. In *AIAA Scitech*, number AIAA 2014-0119, 2014.

[21] Benedikt König and Ehab Fares. Exa powerflow simulations for the sixth aiaa drag prediction workshop. *J. Aircraft*, 55(4), 2018.

[22] CD-adapco Fred Mendonça. BANC-PDCC Gulfstream G550 NLG 1⁄4-scale Simulation using STAR-CCM+. Presentation, 2010.

[23] Thomas R. O. Wainwright, Daniel J. Poole, Christian B. Allen, J. Appa, and O. Darbyshire. High-fidelity aero-structural simulation of occluded wind turbine blades. In *AIAA Scitech 20221 Forum*, 2021.

[24] C. L. Rumsey, J. P. Slotnick, and A. J. Sclafani. Overview and summary of the third aiaa high lift prediction workshop. *J. Aircraft*, 2018.

[25] F. Grimm, G. Reichling, R. Ewert, J. Dierke, B. Noll, and M. Aigner. Stochastic and direct combustion noise simulation of a gas turbine model combustor. *Acta Acustica united with Acustica*, 103(14):262–275, 2017.

[26] Eric Manoha and Bastien Caruelle. Summary of the lagoon solutions from the benchmark problesm for airframe noise compuations-iii workshop. In *21st AIAA/CEAS Aeroacoustics Conference*. AIAA Aviation, 2015.